Coherent tunneling in Cu²⁺- and Ag²⁺-doped MgO and CaO:Cu²⁺ explored through *ab initio* calculations

P. García-Fernández,[1] C. Sousa,[2] J. A. Aramburu,[1] M. T. Barriuso,[3] and M. Moreno[1]

[1]*Departamento de Ciencias de la Tierra y Física de la Materia Condensada, Universidad de Cantabria, 39005 Santander, Spain*
[2]*Departament de Química Física i Centre Especial de Recerca en Química Teórica, Universitat de Barcelona, 08028 Barcelona, Spain*
[3]*Departamento de Física Moderna, Universidad de Cantabria, 39005 Santander, Spain*

The observation of coherent tunnelling in Cu²⁺- and Ag²⁺-doped MgO and CaO:Cu²⁺ was a crucial discovery in the realm of the Jahn-Teller (JT) effect. The main reasons favoring this dynamic behavior are now clarified through *ab initio* calculations on Cu²⁺- and Ag²⁺-doped cubic oxides. Small JT distortions and an unexpected low anharmonicity of the e_g JT mode are behind energy barriers smaller than 25 cm⁻¹ derived through CASPT2 calculations for Cu²⁺- and Ag²⁺-doped MgO and CaO:Cu²⁺. The low anharmonicity is shown to come from a strong vibrational coupling of MO_6^{10-} units ($M=Cu,Ag$) to the host lattice. The average distance between the d^9 impurity and ligands is found to vary significantly on passing from MgO to SrO following to a good extent the lattice parameter.

I. INTRODUCTION

It is well known that the existence of a static or dynamic Jahn-Teller (JT) effect in many transition metal oxides plays a key role for understanding its properties. So, the colossal magnetoresistance found in some manganites is believed to be a consequence of the interplay between a double exchange mechanism and the JT electron-phonon coupling.[1] As another relevant example, the formation of JT polarons has recently been proposed as a possible basis for a superconductivity mechanism in cuprates.[2] A better insight into these issues requires first to elucidate the origin of the coherent tunnelling among equivalent adiabatic minima[3] observed four decades ago in simple systems involving d^9 impurities in cubic oxides like Cu²⁺-doped MgO or CaO.[4] The existence of electron paramagnetic resonance (EPR) spectra displaying a cubic rather than a tetragonal symmetry and showing a dynamic JT effect was a crucial discovery.[4–6] Apart from reflecting the cubic invariance of the $E_g \otimes e_g$ JT coupling such experimental results stressed the key role played by random strains[7] as responsible for static EPR spectra observed for d^9 or d^7 impurities placed substitutionally in cubic halides.[8]

Despite the large amount of experimental information on JT impurities in sixfold coordination there is a crucial question which has not been solved, why a coherent tunnelling occurs for MgO:Cu²⁺ while for Cu²⁺ or Ag²⁺ in SrO a static JT situation is found.[9,6] The present work is aimed to explain this puzzling situation by means of *ab initio* calculations. A good insight into this relevant issue requires to explore the energy barrier, B, between equivalent minima of the $E(Q_\theta \sim 3z^2-r^2; Q_\varepsilon \sim x^2-y^2)$ surface whose microscopic origin is certainly subtle. Indeed no warping appears in the harmonic approximation for a linear JT coupling.[3,8,10]

Aside from the actual value of B there are still doubts about other JT parameters characterizing d^9 impurities in cubic oxides like the JT stabilization energy, E_{JT}. So, Guha and Chase[11] and Reynolds *et al.*[12] estimated E_{JT} in the range

5500–12 000 cm⁻¹ for Cu²⁺- and Ag²⁺-doped MgO and CaO while from the spin-lattice relaxation time, T_1, a much lower value $E_{JT} \approx 300$ cm⁻¹ was derived.[13] In the case of the excited E_g state of MgO:Fe²⁺ Hjortsberg *et al.*[14] estimated $E_{JT} \approx 1300$ cm⁻¹ *assuming* that the separation between the zero-phonon line and the maximum of the associated broad band is just equal to E_{JT}. This figure is thus similar to that reported by Treguenna-Pigot.[15] As regards *ab initio* calculations E_{JT} values in the 300–500 cm⁻¹ range have recently been reported.[10,16]

Searching to improve our knowledge on JT impurities in oxides, *ab initio* electronic structure calculations on Cu²⁺ and Ag²⁺ impurities in cubic oxides as a function of both $Q_\theta = \rho \cos \varphi$ and $Q_\varepsilon = \rho \sin \varphi$ coordinates have been carried out. Particular attention has been addressed to calculate the values of the JT stabilization energy, E_{JT}, and the barrier energy, B, as well as to explore their microscopic origin. Very recently[17] *ab initio* calculations on NaCl:Rh²⁺ and triangular molecules like Cu₃ or Ag₃ have shown that B mainly arises from the anharmonicity of the JT mode. The results obtained in this work have been derived using two different methods in order to reinforce the reliability of present conclusions.

II. THEORY

Following previous works on NaCl:Rh²⁺,[10,17] calculations of 39-ion $MO_6B_{12}O_8B_6O_6^{2-}$ ($M=Cu,Ag$; $B=Mg,Ca,Sr$) clusters centered around the impurity were carried out using the density functional theory (DFT) methodology as implemented in the Amsterdam density functional (ADF) 2000.02 code.[18] The use of finite clusters for describing the properties of these systems is consistent with the highly localized character of the unpaired electron residing solely in the MO_6 complex formed by the impurity and the six nearest O²⁻ anions.[4,6,12] In the present calculations a generalized gradient approximation (GGA) was used for the exchange-correlation functional in the Becke-Perdew form[19] and the basis set of

the best quality in the ADF code was employed. A point charge electrostatic potential was included to take into account the influence of the rest of the ions in the host lattice.

As it is well known, DFT calculations present limitations in the treatment of open shell electronic states, where spin cannot be neglected, so requiring the use of highly correlated calculation methods.[20,17] Taking into account the very subtle effects studied in this work, all DFT results have been complemented by very accurate wave-function-based complete active space perturbation theory of order 2 (CASPT2) calculations as implemented in the MOLCAS 5.3 program.[21] CASPT2 calculations include most of the electronic correlation effects by combining two strategies. In a first step, a correct treatment of the large electron correlation effects in the transition metal d shell is treated in a variational way by constructing an accurate multireference CASSCF wave function for the considered states, with an active space containing nine electrons distributed in all posible ways over 10 orbitals, the five d orbitals of the impurity and a correlating set of five virtual orbitals.[21] In the second step, the remaining (mostly dynamical) electron correlation effects are included by many-body second-order perturbational treatment, CASPT2, taking the CASSCF wave function as the zeroth-order wave function, in which all valence electrons are correlated. Because of the very high computational cost of these calculations, most of the calculations were performed on $MO_6B_6^{4-}$ clusters with only 13 ions. An accurate embedding was constructed surrounding the cluster by *ab initio* model potentials (AIMPs)[22] that take into account the short-range repulsion of the rest of the lattice, and a set of point charges. Moreover, calculations carried out for 25-atom $MO_6B_{12}B_6^{26+}$ clusters did not improve significantly the results derived on the 13-atom clusters.

In the study of JT impurities in cubic crystals it is quite useful to consider first the isotropic distortion produced by a hypothetical ion whose electronic density resembles that of closed shell structure.[10,17,23] This leads to an impurity-ligand distance, R_{oct}, different from R_0 corresponding to the perfect host lattice. In DFT an electronic density displaying cubic symmetry can easily be built for a d^9 impurity through the $(3z^2-r^2)^{1.5}(x^2-y^2)^{1.5}$ configuration.[10,17,23] In a second step, adiabatic calculations are carried out for both $(3z^2-r^2)^2(x^2-y^2)^1$ and $(x^2-y^2)^2(3z^2-r^2)^1$ configurations as a function of the two Q_θ and Q_ε coordinates. For instance, under a $Q_\theta = \sqrt{12}u$ deformation, axial and equatorial metal-ligand distances are given by $R_{ax}=R_{oct}+2u$ and $R_{eq}=R_{oct}-u$, respectively.

By means of these calculations the *parameters* involved in the usual effective Hamiltonian, H_{eff}, describing the $E_g \otimes e_g$ JT effect *within* the $\{x^2-y^2, 3z^2-r^2\}$ basis can be derived and related to the equilibrium geometry at adiabatic minima. H_{eff} is usually written as

$$H_{eff} = V_{1e}\{\mathbf{U}_\theta Q_\theta + \mathbf{U}_\varepsilon Q_\varepsilon\} + \mathbf{I}V_{2a}(Q_\theta^2 + Q_\varepsilon^2)$$
$$+ \mathbf{I}V_{3a}(Q_\theta^3 - 3Q_\theta Q_\varepsilon^2) + V_{2e}\{\mathbf{U}_\theta(Q_\varepsilon^2 - Q_\theta^2) + 2\mathbf{U}_\varepsilon Q_\theta Q_\varepsilon\}. \quad (1)$$

Here $\mathbf{U}_\theta$ and $\mathbf{U}_\varepsilon$ are 2×2 Pauli matrices[7,8] and $\mathbf{I}$ means the identity matrix. The first term in (1) denotes the *linear* JT

coupling while the second and third ones are the elastic and anharmonic contributions, respectively.[3,7,8] V_{2a} is related to the angular frequency of the e_g mode, ω_e, by $M_L\omega_e^2 = 2V_{2a}$, where M_L is the ligand mass. The fourth term depicts the so-called quadratic JT coupling. Recent results[10,17,24] have demonstrated that this contribution plays a minor role for explaining the barrier compared to the anharmonic term. For instance, the relative contribution of the anharmonicity to the barrier is found to be equal to $\sim$98% and $\sim$70% for $CaO:Cu^{2+}$ and $SrO:Cu^{2+}$, respectively.[24] For this reason the quadratic JT coupling will not be considered in the subsequent analysis mainly devoted to explore the sign and absolute value of the anharmonic constant, V_{3a}.

The expansion described in (1) is reasonable provided $\rho_0 \ll \sqrt{12}R_{oct}$ at adiabatic minima, a condition which is usually followed by JT impurities.[10] If only the two first terms in (1) are considered it is found:[3,7,8]

$$\rho_0 = |V_{1e}|/2V_{2a}, \quad E_{JT} = E_{JT}^0 = (1/4)(V_{1e})^2/V_{2a} \quad (2)$$

implying that warping in $E(\rho_0, \varphi)$ depends on the V_{3a} term in (1). When this is taken into account the adiabatic energy of the two solutions of H_{eff} can be approximated by[17]

$$E_-(\rho_0, \varphi) \approx E_0 - E_{JT}^0 + A\cos 3\varphi,$$

$$E_+(\rho_0, \varphi) \approx E_0 + 3E_{JT}^0 + A\cos 3\varphi, \quad (3)$$

where $A \approx V_{3a}\rho_0^3$. Equation (3) means that adiabatic minima in the ground state display a tetragonal symmetry. If $A>0$ ($A<0$) then the equilibrium geometry at the three adiabatic minima corresponds to a compressed (elongated) octahedron. The energy barrier between a compressed $[3\varphi=(2p+1)\pi, p=\text{integer}]$ and an elongated $(3\varphi=2\pi p)$ geometry in the ground state is just equal to $2A$. Around a minimum, $E_-(\rho_0\varphi)$ can be approximated by a harmonic oscillator potential whose associated angular frequency is given by $\omega_c^2 = 9|A|/(M_L\rho_0^2)$. A coherent tunnelling among equivalent adiabatic minima is thus favored if $\omega_c/2 > |B|$.[10] A main goal of the present calculations is just to compute the $F = |B|/(\omega_c/2)$ parameter from the previously calculated V_{3a} and ρ_0 values.

III. RESULTS AND DISCUSSION

Consistently with the size of the employed clusters in all present calculations more than 98% of the unpaired electron density is found to reside within the complex formed by the impurity and ligands. Tables I and II gather the parameters for Cu^{2+}- and Ag^{2+}-doped cubic oxides obtained through CASPT2 calculations, which according to previous results[20,17] is the most reliable method for the present systems. For comparison, computed values are also given for $NaCl:Rh^{2+}$ displaying a static JT effect.[25] For the same reason, Table I also includes the DFT values of R_{oct}, ρ_0, E_{JT}, and ω_e, although the poor self-consistent field convergence in the computed $E_\pm(\rho, \varphi)$ curves are prevented in a few cases to obtain reliable values for the parameters collected in Tables I and II.

CASPT2 and DFT values of R_{oct} and ρ_0 given in Table I are reasonably similar although the latter method leads in

TABLE I. Calculated values of R_{oct} and ρ_0 (in Å units) and E_{JT} and $\hbar\omega_e$ (in cm^{-1} units). CASPT2 results are shown in normal characters while DFT ones are shown in italic characters. The experimental metal-ligand distances R_0 (in Å units) for perfect host lattices are given for comparison.

	R_0	R_{oct}	ρ_0	E_{JT}	$\hbar\omega_e$
NaCl:Rh^{2+}	2.820	2.526	0.276	1832	193
		2.532	*0.260*	*1200*	*165*
MgO:Cu^{2+}	2.107	2.147	0.087	494	485
		2.100	*0.080*	*316*	*490*
CaO:Cu^{2+}	2.405	2.324	0.126	567	250
		2.366	*0.154*	*308*	*357*
SrO:Cu^{2+}	2.584	2.459	0.189	914	195
		2.497	*0.152*	*378*	*200*
MgO:Ag^{2+}	2.107	2.197	0.097	674	544
		2.181	*0.069*	*425*	*581*
CaO:Ag^{2+}	2.405	2.494	0.180	874	291
		2.425	*0.087*	*258*	*390*
SrO:Ag^{2+}	2.584	2.543	0.251	1100	255
		2.538		*1100*	*378*

general to smaller values for E_{JT}. A similar pattern was previously obtained through Hartree-Fock calculations.[26] Hence, our results support a E_{JT} value in the range 300–500 cm^{-1} for MgO:Cu^{2+}. A similar value ($E_{JT}=394$ cm^{-1}) has been obtained for the excited ^5E_g state of MgO:Fe^{2+}. The much larger estimate of E_{JT} by Hjortsberg *et al.*[14] can be ascribed to the neglect of the contribution of the symmetric a_{1g} mode to the $\Delta E \approx 1100$ cm^{-1} separation between the electric dipole origin and the maximum of the associated broad band. For transition-metal impurities at octahedral sites $\Delta E \approx S_a\omega_a + S_e\omega_e$,[27] where $E_{JT} \equiv S_e\omega_e$ and $S_e(S_a)$ is the Huang-Rhys factor of the $e_g(a_{1g})$ mode. Present DFT calculations give $S_a\omega_a = 360$ cm^{-1} thus supporting a E_{JT} value again not far from 500 cm^{-1} rather than close to 1500 cm^{-1}.[14] Moreover, the value $V_{2a}=1.85$ eV/Å^2 derived for CaO:Cu^{2+} leads to $\omega_e=250$ cm^{-1} which is not far from the Raman peak estimated at ~300 cm^{-1}.[11]

TABLE II. Values of coupling constants V_{1e}, V_{2a}, and V_{3a}, energy barrier B, and $F=|B|/(\omega_c/2)$ and $E_{JT}/\hbar\omega_e$ ratios obtained by means of CASPT2 calculations. Units of $V_{i\gamma}$ are eV/Å^i while B is in cm^{-1}. If $B>0$ the minimum corresponds to a compressed configuration and the top of the barrier to an elongated one. The opposite happens for $B<0$.

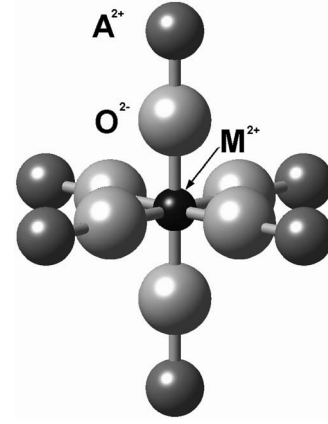| System	V_{1e}	V_{2a}	V_{3a}	B	F	$E_{JT}/\hbar\omega_e$
NaCl:Rh^{2+}	1.42	2.70	−1.248	−511	6.388	9.492
MgO:Cu^{2+}	1.08	6.97	0.651	4	0.114	1.019
CaO:Cu^{2+}	0.52	1.85	0.654	20	0.397	2.268
SrO:Cu^{2+}	0.51	1.12	0.934	98	2.357	4.687
MgO:Ag^{2+}	1.73	8.79	0.442	−18	0.316	1.239
CaO:Ag^{2+}	1.06	2.52	$\sim$1.0	52	1.427	3.003
SrO:Ag^{2+}	0.97	1.91	0.292	71	2.125	4.313

FIG. 1. Cluster of 13 ions used in the CASPT2 calculations of $AO:M^{2+}$ ($A=$Mg, Ca, Sr; $M=$Cu, Ag) systems.

Let us now focus on calculated parameters in Table II whose main features are the following: (i) The values of $|B|$ obtained for Cu^{2+}- and Ag^{2+}-doped MgO and CaO:Cu^{2+} are smaller than 20 cm^{-1} and thus at least 25 times smaller than the figure derived for NaCl:Rh^{2+}. (ii) The F parameter is found to be smaller than 0.4 for Cu^{2+}- and Ag^{2+}-doped MgO and CaO:Cu^{2+}, while it is equal to 6.4 for NaCl:Rh^{2+}. (iii) On passing from a MgO to a SrO host lattice F increases by a factor equal to 20 and 7 for Cu^{2+} and Ag^{2+} impurities, respectively. These trends strongly support that MgO is a more suitable host lattice than SrO for observing dynamic EPR spectra of d^9 ions in agreement with experimental facts.[4,6,9] (iv) Similarly to the results obtained for NaCl:Rh^{2+},[10] the barrier B is found to be dominated by the anharmonic contribution for Cu^{2+} and Ag^{2+} in cubic oxides. However, the *sign* of B and V_{3a} in the latter cases is in general *opposite* to that encountered in NaCl:Rh^{2+} where the elongated RhCl$_6^{4-}$ complex has been demonstrated to be *significantly decoupled* from the rest of the host lattice.[10] (v) The evolution of E_{JT}/ω_e in Table II exhibits a similar trend as the F parameter. However, direct information about the barrier is only embodied in the last parameter.

A microscopic explanation of the main trends of B and F requires a detailed analysis of the equilibrium geometry displayed in Table I. First, it can be noticed that the calculated R_{oct} distances follow rather closely the value of R_0, the differences between R_{oct} and R_0 being less than 5%. Therefore, according to the theory of elasticity, the second neighbors A^{2+} ($A=$Mg, Ca or Sr) in $\langle 100 \rangle$ directions (Fig. 1) are expected to be shifted by less than 1%. This argument justifies *a posteriori* our previous assumption to keep A^{2+} ions at the host lattice positions. It is worth stressing that results in Table I are *qualitatively different* from those for impurities in halide lattices. In these systems R_{oct} is essentially determined by the relative size of impurity and ligand and only slightly dependent on the host lattice. This idea can be quantified by means of the parameter $f=\Delta R_{oct}/\Delta R_0$, the ratio of the variations of R_0 and R_{oct} induced by a change of host lattice. For Cr^{3+} in elpasolites[28] or Fe^{3+} in fluoroperovskites[29] f has been determined to be ≤ 0.1 while a value $f=0.3$ reflects the behavior of Mn^{2+} impurities in cubic fluoroperovskites.[27] For Cu^{2+} and Ag^{2+} in cubic oxides f values derived from Table I
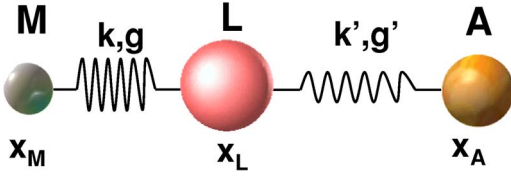
FIG. 2. (Color online) Model representing three atoms (M=impurity metal ion, L=oxygen ligand, and A=next neighbor in the $\langle 100 \rangle$ direction) connected by two springs with parameters (k,g) and (k',g'), respectively. x_i represents the position of atom i.

lie in the 0.6–0.8 range. This strongly suggests that the interaction of the ligand ion with the nearest A^{2+} cation of the host lattice (Fig. 1) dominates over the impurity-ligand interaction. In a ball-and-spring model (Fig. 2) the energy of a given M^{2+}-O^{2-}-A^{2+} bond in Fig. 1 is given by[27]

$$E = E_0 + (1/2)k(x_L - x_M - r_0)^2 + (1/2)k(x_A - x_L - r_0')^2$$
$$+ (1/6)g(x_L - x_M - r_0)^3 + (1/6)g'(x_A - x_L - r_0')^3, \quad (4)$$

where x_M, x_L, and x_A mean the position of the impurity, the ligand and the A^{2+} ion lying in the same $\langle 100 \rangle$ direction, respectively, while r_0 and r_0' are parameters describing the two springs. If the impurity and the A^{2+} ion are fixed the energy changes induced by variations of the ligand around the equilibrium position, x_{L0}, can be approximately described by

$$E \approx E_0 + (1/2)(k + k')(x_L - x_{L0})^2 + (1/6)(g - g')(x_L - x_{L0})^3. \quad (5)$$

Calculated values of the k/k' ratio for the present systems are collected in Table III. The value $k/k' = 2.5$ found for NaCl:Rh^{2+} indicates a significant *decoupling* of the RhCl$_6^{4-}$ complex from the ions of the host lattice. By contrast the vibrational coupling of CuO$_6^{10-}$ units (where active electrons reside) to the host lattice is, as expected, much stronger, the k/k' values lying around 0.4. In fact, for cases like MgO:Cu^{2+} (but not for NaCl:Rh^{2+}) the impurity and the host cation have the same nominal charge.

B and F values are greatly sensitive to ρ_0 which in turn depends on the ratio V_{1e}/V_{2a} [Eq. (2)]. Although, as expected, both V_{1e} and V_{2a} decrease on passing from MgO to SrO, the ratio V_{1e}/V_{2a} and thus ρ_0 experience a significant increase. This fact is quite consistent with the well-known increase of the Huang-Rhys factors S_a and S_e when R_0 increases,[27,30] explored first in Ref. 31. For instance S_e^2 is

TABLE III. Values of harmonic force constants k and k' (in eV/Å^2) from DFT calculations.

System	k	k'	k/k'
NaCl:Rh^{2+}	4.12	1.64	2.53
MgO:Cu^{2+}	5.12	15.40	0.33
MgO:Ag^{2+}	8.60	16.08	0.52
SrO:Cu^{2+}	2.68	5.96	0.45
SrO:Ag^{2+}	4.16	5.52	0.75

proportional to $V_{1e}/\omega_e^{3/2}$.[27] A similar behavior has also been observed[32,27] for the Stokes shift (depending on $2S_a\omega_a + 2S_e\omega_e$) and is thus consistent with the increase of E_{JT} on going from MgO to SrO.

Although the important increase of ρ_0 along the MgO$\rightarrow$CaO$\rightarrow$SrO host lattices favors a transition from a dynamic to a static regime it is also crucial to consider the influence of the anharmonic constant V_{3a} on both B and F. As shown in Table II, on passing from NaCl:Rh^{2+} to MgO:Cu^{2+} V_{2a} increases by a factor of 3 while $|V_{3a}|$ *decreases* by a factor of 2. Moreover $V_{3a} < 0$ for the former system while $V_{3a} > 0$ for the latter. According to Eq. (5) V_{3a} is proportional to the *difference* between the two anharmonic constants g and g' that are negative for ordinary bond types. The negative sign of both V_{3a} and B parameters found for NaCl:Rh^{2+} is consistent with the relevant decoupling of RhCl$_6^{4-}$ from the rest of the lattice.[10] In addition, the anharmonicity of the Rh—Cl bond contributes to the higher stability of the elongated over the compressed form of the RhCl$_6$ octahedron. On the contrary, if the relative importance of k' increases, V_{3a} is expected to be *softened* and can even experience a *change of sign* leading to positive B values. The small k/k' ratio in Table III for SrO:Cu^{2+} is accompanied by a rather large, positive V_{3a} and a sizeable $B = +98$ cm^{-1}. Hence, the interpretation of our theoretical result based on the ball-and-spring model supports the existence of a compressed equilibrium geometry as demonstrated in the static EPR spectrum of SrO:Cu^{2+}.[9] Similar observations hold for CaO:Cu^{2+}, for which the same equilibrium geometry has been inferred from the Raman spectra corresponding to vibronic levels.[11]

Passing from first-row to second-row transition-metal ions in general more covalent bonds are formed. So, it can be expected that the replacement of the $3d$ Cu^{2+} ion for the $4d$ ion Ag^{2+} increases the relative importance of the impurity-ligand constant k. We obtain a k/k' ratio of 0.75 for SrO:Ag^{2+}, which is the largest value found in all six systems studied here (Table III). In agreement with this, we find a very small V_{3a} value, close to zero, i.e., at the border of the inversion of the relative stability of elongated and compressed forms of the AgO$_6^{10-}$ complex. Nevertheless, B is still found to be positive (71 cm^{-1}) (Table II), whereas experimental EPR data on this system indicate however an elongated octahedral geometry.[6]

IV. FINAL REMARKS

The present results, together with those recently obtained on layered perovskites,[23] stress the importance of *ab initio* calculations for gaining a better insight into the subtle phenomena related to the JT effect. This is particularly true as regards the barrier energy, B, on which the experimental information is certainly scarce. This parameter plays a key role for the existence of coherent tunnelling, whose relevance for quantum information processing has recently been pointed out.[33] It is worth noting that static situations can experimentally be found even if $F \ll 1$. It was first pointed out by Ham[7] that defects can destroy the coherence and lock at $T=0$ K the wave function in the lowest potential well. In this sense

remote defects leading to energy differences among the three wells of only $\sim 1-10$ cm^{-1} can suffice for producing a static situation.

As a main conclusion, it has been shown in this work that both the sign of V_{3a} and the nature of the ground state can be modified simply by considering the elastic coupling of the complex to the rest of the lattice. Another relevant result concerns the variation of the average impurity-ligand distance along the series of cubic oxides. While for transition-metal impurities in fluorides or chlorides with sixfold coordination the impurity-ligand distance is usually close to the sum of ionic radii,[27,29] for present cases it follows the host lattic parameter. This different behavior can be related to the bigger deformability of the O^{2-} ion in comparison to more rigid ions like F$^-$ or Cl$^-$.[34] As the electronic properties associated with the impurity essentially depend on the actual value of the impurity-ligand distance it can be expected[35] that the charge transfer transitions undergo a strong redshift on passing from MgO : Cu^{2+} to SrO : Cu^{2+}. Further work along this line is underway.

[1] A. J. Millis, B. I. Shraiman, and R. Mueller, Phys. Rev. Lett. **77**, 175 (1996); A. J. Millis, Nature (London) **392**, 147 (1998).

[2] V. V. Kabanov and D. Mihailovic, Phys. Rev. B **65**, 212508 (2002).

[3] I. Bersuker and V. Polinger, in *Vibronic Interactions in Molecules and Crystals* (Springer-Verlag, Berlin, 1989).

[4] R. E. Coffman, Phys. Lett. **21**, 381 (1966); R. E. Coffman, D. L. Lyle, and D. R. Mattison, J. Phys. Chem. **72**, 1392 (1968).

[5] U. Höchli and T. L. Estle, Phys. Rev. Lett. **18**, 128 (1968).

[6] L. A. Boatner, R. W. Reynolds, M. M. Abraham, and Y. Chen, Phys. Rev. Lett. **31**, 7 (1973).

[7] F. S. Ham, in *Electron Paramagnetic Resonance*, edited by S. Geschwind (Plenum, New York, 1972).

[8] H. Bill, in *The Dynamical Jahn-Teller Effect in Localized Systems*, edited by Yu. E. Perlin and M. Wagner (Elsevier, Amsterdam, 1984).

[9] Yu. N. Tolparov, G. L. Bir, L. S. Sochava, and N. N. Kovalev, Sov. Phys. Solid State **16**, 573 (1974).

[10] J. A. Aramburu, M. T. Barriuso, P. García-Fernández, and M. Moreno, Adv. Quantum Chem. **44**, 446 (2003).

[11] S. Guha and L. L. Chase, Phys. Rev. B **12**, 1658 (1974).

[12] W. Reynolds, L. Boatner, M. Abraham, and Y. Chen, Phys. Rev. B **10**, 3802 (1974).

[13] U. Höchli, K. A. Müller, and P. Wysling, Phys. Lett. **15**, 5 (1965).

[14] A. Hjortsberg, B. Nygren, J. Vallin, and F. S. Ham, Phys. Rev. Lett. **39**, 1233 (1977).

[15] Ph. L. W Tregenna-Piggott, Adv. Quantum Chem. **44**, 446 (2003).

[16] J. L. Pascual, B. Savoini, and R. Gonzalez, Phys. Rev. B **70**, 045109 (2004).

[17] P. García-Fernández, I. B. Bersuker, J. A. Aramburu, M. T. Barriuso, and M. Moreno, Phys. Rev. B **71**, 184117 (2005).

[18] G. te Velde, F. M. Bickelhaupt, E. J. Baerends, C. Fonseca Guerra, S. J. A. van Gisbergen, J. G. Snijders, and T. Ziegler, J. Comput. Chem. **22**, 931 (2001).

[19] A. D. Becke, Phys. Rev. A **38**, 3098 (1988); J. P. Perdew, Phys. Rev. B **33**, 8822 (1986).

[20] A. Ramirez-Solis and J. P. Daudey, J. Chem. Phys. **120**, 3221 (2004); L. Hozoi, A. H. de Vries, A. B. van Oosten, R. Broer, J. Cabrero, and C. de Graaf, Phys. Rev. Lett. **89**, 076407 (2002); F. Illas, I. de P. R. Moreira, J. M. Bofill, and M. Filatov, Phys. Rev. B **70**, 132414 (2004); A. Gellé, M. L. Munzarova, M.-B. Lepetit, and F. Illas, *ibid.* **68**, 125103 (2003).

[21] B. O. Roos, K. Andersson, M. P. Fülscher, P.-A. Malmqvist, L. Serrano-Andrés, K. Pierloot, and M. Merchán, Adv. Chem. Phys. **93**, 219 (1996).

[22] L. Seijo and Z. Barandiarán, in *Computational Chemistry: Reviews of Current Trends*, edited by J. Leszczynski (World Scientific, Singapore, 1999).

[23] J. M. García-Lastra, J. A. Aramburu, M. T. Barriuso, and M. Moreno, Phys. Rev. Lett. **93**, 226402 (2004).

[24] P. García-Fernández, thesis, University of Cantabria, 2004.

[25] H. Vercammen, D. Schoemaker, B. Briat, F. Ramaz, and F. Callens, Phys. Rev. B **59**, 11286 (1999).

[26] J. L. Pascual, L. Seijo, and Z. Barandiarán, J. Chem. Phys. **98**, 9715 (1993).

[27] M. T. Barriuso, M. Moreno, and J. A. Aramburu, Phys. Rev. B **65**, 064441 (2002).

[28] J. A. Aramburu, M. Moreno, K. Doclo, C. Daul, and M. T. Barriuso, J. Chem. Phys. **110**, 1497 (1999).

[29] J. A. Aramburu, J. I. Paredes, M. T. Barriuso, and M. Moreno, Phys. Rev. B **61**, 6525 (2000).

[30] O. S. Wenger, R. Valiente, and H. U. Güdel, J. Chem. Phys. **115**, 3819 (2001).

[31] M. Moreno, M. T. Barriuso, and J. A. Aramburu, J. Phys.: Condens. Matter **4**, 9481 (1992).

[32] M. C. Marco de Lucas, F. Rodríguez, and M. Moreno, Phys. Rev. B **50**, 2760 (1994).

[33] A. M. Stoneham, Phys. Status Solidi C **2**, 25 (2005).

[34] A. Martín Pendás, A. Costales, M. A. Blanco, J. M. Recio, and V. Luaña, Phys. Rev. B **62**, 13970 (2000).

[35] M. Moreno, J. A. Aramburu, and M. T. Barriuso, Struct. Bonding (Berlin) **106**, 127 (2004).